Memoirs of the Faculty of Engineering, Okayama University, Vol. 42, pp. 79-90, January 2008

Temperature Distribution Control of Reactor Furnace by State Space Method using FEM Modeling

Tadafumi NOTSU *
Division of Electronic and
Information System Engineering
Graduate School of Natural Science and Technology
Okayama University
3-1-1, Tsushima-Naka Okayama, 700-8530

Masami KONISHI
Division of Industrial Innovation Science
Graduate School of Natural Science and Technology
Okayama University
3-1-1, Tsushima-Naka Okayama, 700-8530

Jun IMAI
Division of Industrial Innovation Science
Graduate School of Natural Science and Technology
Okayama University
3-1-1, Tsushima-Naka Okayama, 700-8530

(Received December 12, 2007)

The operations of a reactor furnace such as a blast furnace still depend on the experiences and intuitions of skilled operators due to the complexity of internal furnace phenomena and high temperature. There is a great demand for stable operations under the circumstances of a decrease in the number of skilled operators and difficulty in technology inheritance. This paper aims to construct mathematical description for control of a reactor furnace. Further, the linear-quadratic-gaussian control system for a reactor furnace is proposed, which estimates inner furnace temperature distribution using measured data near furnace wall. Temperature distribution of a furnace is controlled based on the estimated inner temperature distribution changing of boundary conditions of a furnace. The practicability of the proposed control method was checked through numerical experiments.

1 INTRODUCTION

A reactor furnace such as a blast furnace have been playing vital roles in steel industry. The performance of a furnace has been improved remarkably accompanying enlargement of furnace facilities and expanding production. However, the operations of a furnace still depend on the experiences and intuitions of skilled operators because of the complexity of internal furnace phenomena and high temperature. There are various factors governing such as gas flow, chemical reactions, burn-through and anastomoses of iron ores and movement of fillings in a furnace.

Stable operations of blast furnace are strongly required from difficulties in furnace regulation. Recently, there occurred a great demand for automated operations accompanied with decrease in the number of skilled operators and difficulty in technology inheritance.

In this research, we pursue the construction of control system for a reactor furnace that estimates and

*notsu@cntr.elec.okayama-u.ac.jp

controls temperature distribution in the reactor furnace. As mentioned, a reactor furnace has complex phenomena such as chemical reactions, high pressure and high temperature internally. Variables only near the furnace wall can be measured and can be used for furnace control. Because a reactor furnace is huge size and the internal situation of the furnace can't be changed directly. Therefore, control system that estimated inner temperature distribution of a furnace from the measured data near the furnace wall and controlled temperature distribution of a furnace based on the estimated inner temperature distribution changing of boundary conditions of a furnace was constructed.

First, the reactor furnace simulator is constructed, which treats gas flow and temperature distribution in the furnace. The numerically simulated furnace has instrumentations only near the furnace wall and control inputs can be operated only at boundaries. This research carried out by using the reactor furnace simulator. To make the control system design, state space model is derived by applying finite element method (FEM) to the reactor furnace simulator. Through this procedure, linear control theory is applied for design of control system. Further, linear-quadratic-gaussian (LQG) control is adopted in order to deal with the problem description. Details are described in the following sections.

2 REACTOR FURNACE MODEL

Blast furnaces are used when pig irons are made from iron ores. Schematic of a blast furnace is shown in Fig.1. The height of a blast furnace is about 40 meters and the diameter of it is about 20 meters. Iron ores and cokes are charged alternately from upper part of a blast furnace. Moreover, there are multiple tuyeres at the bottom of a blast furnace and blasts of hot air of about 1200 degrees C are blown through these tuyeres. Cokes burn and carbon monoxide is generated by the blasts of hot air. Iron ores are reduced to pig irons in about 8 hours by the reaction with the carbon monoxide and pig irons accumulate at the bottom of a blast furnace. On the other hand, the blasts of hot air are discharged from upper part of a blast furnace.

As we have mentioned above, a blast furnace has complex phenomena such as chemical reactions, high pressure and high temperature internally. Therefore, instrumentations of a blast furnace can be located only near the furnace wall.

In the following, reactor furnace model will be constructed.

Two-dimensional reactor furnace model is shown in Fig.2, where $U_{\text{in}1}$, $U_{\text{in}2}$, $V_{\text{in}1}$ and $V_{\text{in}2}$ are velocity of blowing gases from tuyeres. Also, node number (i, j) is assigned to node point as shown in Fig.2. Furthermore, features of reactor furnace model are shown Table.1.

Instrumentations are set up as shown in Fig.3, where $\triangle$ is gas flow meter and $\square$ is solid thermometer. These instrumentations are set up along the outside of reactor furnace model and the top of solid layer.

Suppose that pressure distribution is $P(x, y, t)$, gas flow distribution is

$$\boldsymbol{V}(x, y, t) = U(x, y, t)\boldsymbol{i} + V(x, y, t)\boldsymbol{j}, \tag{1}$$

gas temperature distribution is $T_g(x, y, t)$ and solid temperature distribution is $T_s(x, y, t)$ in reactor furnace model. These variables are discretized by using node number (i, j) and time n as shown in Table.2.

Reactor furnace model calculates the discrete values shown in Table.2 by applying MAC method and finite-difference method[1] to governing equation of P, $\boldsymbol{V}$, T_g and T_s in the following subsection.

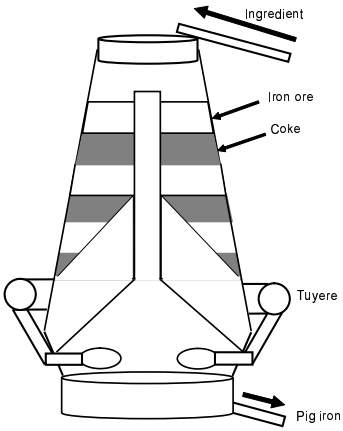

Fig. 1: Schematic of a blast furnace

Table. 1: Features of reactor furnace model

node numbers of i	13
node numbers of j	21
node number (i,j) of outlet	(6,21) (7,21) (8,21)
node number (i,j) of inlet	(4,1) (10,1) (1,3) (13,3)

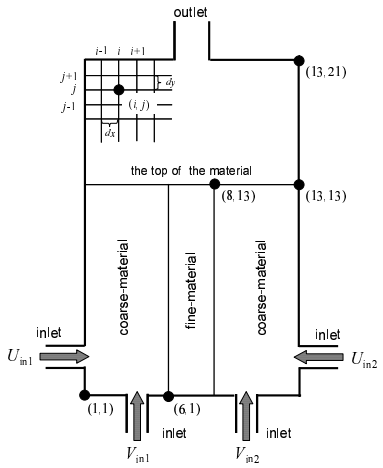

Fig. 2: Two-dimensional reactor furnace model

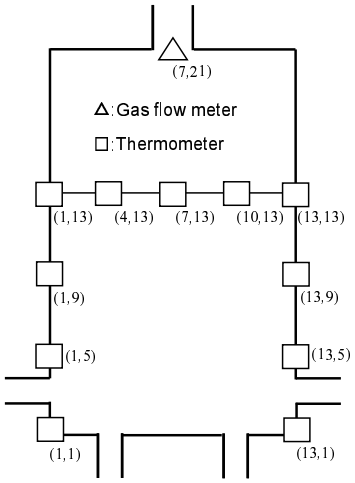

Fig. 3: Instrumentations

Table. 2: Variables of node number (i,j) at n

$\boldsymbol{V}(x,y,t)$	$U^n_{i,j}$, $V^n_{i,j}$
$P(x,y,t)$	$P^n_{i,j}$
$T_g(x,y,t)$	$T_g{}^n_{i,j}$
$T_s(x,y,t)$	$T_s{}^n_{i,j}$

2.1 Gas Flow Model[2, 3, 4, 5]

Assuming that pressure and gas flow are described by the equation of continuity and the Navier-Stokes equation added the Erugan equation[6, 7], we get

$$\frac{\partial U}{\partial x}+\frac{\partial V}{\partial y}=0 \tag{2}$$

$$\frac{\partial U}{\partial t}=-\left(U\frac{\partial U}{\partial x}+V\frac{\partial U}{\partial y}\right)-\frac{\partial P}{\partial x} +\frac{1}{\mathrm{Re}}\left(\frac{\partial^2 U}{\partial x^2}+\frac{\partial^2 U}{\partial y^2}\right)-\left(f_1+f_2\sqrt{U^2+V^2}\right)U \tag{3}$$

$$\frac{\partial V}{\partial t}=-\left(U\frac{\partial V}{\partial x}+V\frac{\partial V}{\partial y}\right)-\frac{\partial P}{\partial y} +\frac{1}{\mathrm{Re}}\left(\frac{\partial^2 V}{\partial x^2}+\frac{\partial^2 V}{\partial y^2}\right)-\left(f_1+f_2\sqrt{U^2+V^2}\right)V \tag{4}$$

Boundary conditions hold

- Furnace bottom and wall

$$U=V=0,\ \frac{\partial P}{\partial n}=0\ \ n:\text{normal vector} \tag{5}$$

- Outlet

$$U^n_{i,21}=U^n_{i,20},\ V^n_{i,21}=V^n_{i,20},\\ P^n_{i,21}=0\ (i=6,7,8) \tag{6}$$

- Inlet

$$U^n_{1,3}=U_{\mathrm{in1}},\ U^n_{13,3}=U_{\mathrm{in2}},\\ V^n_{4,1}=V_{\mathrm{in1}},\ V^n_{10,1}=V_{\mathrm{in2}} \tag{7}$$

where P is pressure distribution, $\boldsymbol{V}$ is gas flow distribution, Re is Reynolds number, f_1 and f_2 are coefficients of the Erugan equation, U_{in1}, U_{in2}, V_{in1} and V_{in2} are velocity of blowing gases from tuyeres.

2.2 Gas Temperature Model[2, 3, 4, 5]

Assuming that gas temperature is described by energy equation added heat transfer between solid and gas[6], we get

$$\frac{\partial T_g}{\partial t}=-U\frac{\partial T_g}{\partial x}-V\frac{\partial T_g}{\partial y}+\frac{1}{\mathrm{RePr}}\left(\frac{\partial^2 T_g}{\partial x^2}+\frac{\partial^2 T_g}{\partial y^2}\right) -\alpha(T_g-T_s) \tag{8}$$

Boundary conditions hold

- Furnace bottom

$$\frac{\partial T_g}{\partial y}=0 \tag{9}$$

- Wall and outlet

$$\frac{\partial T_g}{\partial n}=a(T_g-T_{\mathrm{out}})\ \ n:\text{normal vector} \tag{10}$$

- Inlet

$$T_g{}^{n}_{1,3} = T_{g\ \mathrm{in1}},\ T_g{}^{n}_{13,3} = T_{g\ \mathrm{in2}},$$
$$T_g{}^{n}_{4,1} = T_{g\ \mathrm{in3}},\ T_g{}^{n}_{10,1} = T_{g\ \mathrm{in4}} \tag{11}$$

where T_g is gas temperature distribution, T_s is solid temperature distribution, Pr is Prandtl number, α and a are coefficients of heat transfer, T_{out} is external temperature, $T_{g\ \mathrm{in1}}$, $T_{g\ \mathrm{in2}}$, $T_{g\ \mathrm{in3}}$ and $T_{g\ \mathrm{in4}}$ are temperature of blowing gases from tuyeres.

2.3 Solid Temperature Model[2, 3, 4, 5]

Assuming that solid temperature is described by heat conduction equation added reaction heat of material and heat transfer between gas and solid[8], we get

$$\frac{\partial T_s}{\partial t} = \beta\left(\frac{\partial^2 T_s}{\partial x^2} + \frac{\partial^2 T_s}{\partial y^2}\right) - \gamma(T_s - T_g) + f_3(U, V, T_g) \tag{12}$$

Boundary conditions hold

- Furnace bottom

$$\frac{\partial T_s}{\partial y} = 0 \tag{13}$$

- Top of solid layer

$$\frac{\partial T_s}{\partial y} = -b_{\mathrm{up}}(T_s - T_g) \tag{14}$$

- Wall

$$\frac{\partial T_s}{\partial n} = b(T_s - T_{\mathrm{out}}) \quad n : \text{normal vector} \tag{15}$$

where β, γ, b_{up} and b are coefficients of heat transfer, f_3 is reaction heat of material. f_3 is the following

$$f_3(U, V, T_g) = \frac{Q_1}{D_p}\frac{\exp\{-E/(R \cdot T_g)\}}{1 + \exp\{(T_g - 1000)/K_1\}} \times Q_2\sqrt{U^2 + V^2} \tag{16}$$

where D_p is diameter of material particle, Q_1, Q_2, E, R and K_1 are constant.

3 DERIVATION OF STATE SPACE MODEL

In this section, state space model will be constructed based on (2)-(16). State space model represents characteristic of desired distribution neighborhood and consists of state equation and output equation. If state space model is derived, linear control theory[9, 10, 11] becomes available.

First, linearized equations are derived by using (2)-(16) and desired distribution. Then, descriptor system is derived by applying FEM to the linearized equations. Next, state equation is derived by applying generalized inverse matrix to the descriptor system. Finally, output equation is constructed by instrument placement shown in Fig.3. Through this procedure, state space model is constructed.

3.1 Linearization of Desired Distribution Neighborhood[12]

A steady state solution of (2)-(16) is shown in Fig.4-7 under the condition of appendix A.

Suppose that a steady state solution shown in Fig.4-7 is desired distribution (P_r, $\boldsymbol{V}_r$, $T_{g\ r}$, $T_{s\ r}$) and constant velocity of blowing gases from tuyeres for desired distribution is ($\tilde{U}_{\mathrm{in1}}$, $\tilde{U}_{\mathrm{in2}}$, $\tilde{V}_{\mathrm{in1}}$, $\tilde{V}_{\mathrm{in2}}$). Defining the perturbation variables (ΔP, ΔU, ΔV, ΔT_g, ΔT_s) and (ΔU_{in1}, ΔU_{in2}, ΔV_{in1}, ΔV_{in2}) as

$$P = P_r + \Delta P, \quad U = U_r + \Delta U, \quad V = V_r + \Delta V$$
$$T_g = T_{g\ r} + \Delta T_g, \quad T_s = T_{s\ r} + \Delta T_s \tag{17}$$

$$U_{\mathrm{in1}} = \tilde{U}_{\mathrm{in1}} + \Delta U_{\mathrm{in1}}, \quad U_{\mathrm{in2}} = \tilde{U}_{\mathrm{in2}} + \Delta U_{\mathrm{in2}}$$
$$V_{\mathrm{in1}} = \tilde{V}_{\mathrm{in1}} + \Delta V_{\mathrm{in1}}, \quad V_{\mathrm{in2}} = \tilde{V}_{\mathrm{in2}} + \Delta V_{\mathrm{in2}} \tag{18}$$

and inserting into (2)-(16), we get the linearized equations

$$\frac{\partial \Delta U}{\partial x} + \frac{\partial \Delta V}{\partial y} = 0 \tag{19}$$

$$\begin{aligned}\frac{\partial \Delta U}{\partial t} = &-\left(\frac{\partial U_r}{\partial x}\Delta U + U_r\frac{\partial \Delta U}{\partial x}\right.\\ &\left.+\frac{\partial U_r}{\partial y}\Delta V + V_r\frac{\partial \Delta U}{\partial y}\right) - \frac{\partial \Delta P}{\partial x}\\ &+\frac{1}{\mathrm{Re}}\left(\frac{\partial^2 \Delta U}{\partial x^2} + \frac{\partial^2 \Delta U}{\partial y^2}\right) - f_1\Delta U\\ &-f_2\frac{2U_r^2 + V_r^2}{\sqrt{U_r^2 + V_r^2}}\Delta U - f_2\frac{U_r V_r}{\sqrt{U_r^2 + V_r^2}}\Delta V\end{aligned} \tag{20}$$

$$\begin{aligned}\frac{\partial \Delta V}{\partial t} = &-\left(\frac{\partial V_r}{\partial x}\Delta U + U_r\frac{\partial \Delta V}{\partial x}\right.\\ &\left.+\frac{\partial V_r}{\partial y}\Delta V + V_r\frac{\partial \Delta V}{\partial y}\right) - \frac{\partial \Delta P}{\partial y}\\ &+\frac{1}{\mathrm{Re}}\left(\frac{\partial^2 \Delta V}{\partial x^2} + \frac{\partial^2 \Delta V}{\partial y^2}\right) - f_1\Delta V\\ &-f_2\frac{U_r^2 + 2V_r^2}{\sqrt{U_r^2 + V_r^2}}\Delta V - f_2\frac{U_r V_r}{\sqrt{U_r^2 + V_r^2}}\Delta U\end{aligned} \tag{21}$$

Boundary conditions hold

- Furnace bottom

$$\Delta U = \Delta V = 0,\ \frac{\partial \Delta P}{\partial n} = 0 \quad n : \text{normal vector} \tag{22}$$

- Outlet

$$\Delta U^n_{i,21} = \Delta U^n_{i,20},\ \Delta V^n_{i,21} = \Delta V^n_{i,20}$$
$$\Delta P^n_{i,21} = 0\ (i = 6, 7, 8) \tag{23}$$

- Inlet

$$\Delta U^n_{1,3} = \Delta U_{\text{in1}},\ \Delta U^n_{13,3} = \Delta U_{\text{in2}}$$
$$\Delta V^n_{4,1} = \Delta V_{\text{in1}},\ \Delta V^n_{10,1} = \Delta V_{\text{in2}} \tag{24}$$

$$\frac{\partial \Delta T_g}{\partial t} = -\left(\frac{\partial T_{g\,r}}{\partial x}\Delta U + U_r \frac{\partial \Delta T_g}{\partial x} + \frac{\partial T_{g\,r}}{\partial y}\Delta V + V_r \frac{\partial \Delta T_g}{\partial y}\right) + \frac{1}{\text{RePr}}\left(\frac{\partial^2 \Delta T_g}{\partial x^2} + \frac{\partial^2 \Delta T_g}{\partial y^2}\right) - \alpha(\Delta T_g - \Delta T_s) \tag{25}$$

Boundary conditions hold

- Furnace bottom

$$\frac{\partial \Delta T_g}{\partial y} = 0 \tag{26}$$

- Wall and outlet

$$\frac{\partial \Delta T_g}{\partial n} = a \Delta T_g \quad n : \text{normal vector} \tag{27}$$

- Inlet

$$\Delta T_{g\ 1,3}^{\ n} = 0,\ \Delta T_{g\ 13,3}^{\ n} = 0,$$
$$\Delta T_{g\ 4,1}^{\ n} = 0,\ \Delta T_{g\ 10,1}^{\ n} = 0 \tag{28}$$

$$\frac{\partial \Delta T_s}{\partial t} = \beta\left(\frac{\partial^2 \Delta T_s}{\partial x^2} + \frac{\partial^2 \Delta T_s}{\partial y^2}\right) - \gamma(\Delta T_s - \Delta T_g) + \left.\frac{\partial f_3}{\partial U}\right|_{\substack{T_g = T_{gr} \\ U = U_r \\ V = V_r}} \Delta U + \left.\frac{\partial f_3}{\partial V}\right|_{\substack{T_g = T_{gr} \\ U = U_r \\ V = V_r}} \Delta V + \left.\frac{\partial f_3}{\partial T_g}\right|_{\substack{T_g = T_{gr} \\ U = U_r \\ V = V_r}} \Delta T_g \tag{29}$$

Boundary conditions hold

- Furnace bottom

$$\frac{\partial \Delta T_s}{\partial y} = 0 \tag{30}$$

- Top of solid layer

$$\frac{\partial \Delta T_s}{\partial y} = -b_{\text{up}}(\Delta T_s - \Delta T_g) \tag{31}$$

- Wall

$$\frac{\partial \Delta T_s}{\partial n} = b \Delta T_s \tag{32}$$

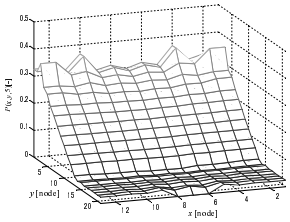

Fig. 4: Steady distribution of pressure ($t = 5[-]$)

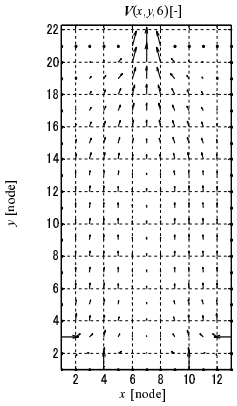

Fig. 5: Steady distribution of gas flow ($t = 6[-]$)

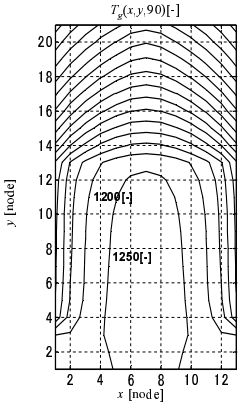

Fig. 6: Steady distribution of gas temperature ($t = 90[-]$)

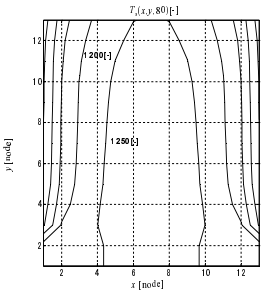

Fig. 7: Steady distribution of solid temperature ($t = 80[-]$)

3.2 Application of FEM to Linearized Equations[13]

In this subsection, FEM is applied to the linearized equations. Defining positions of perturbation variables and triangular elements of FEM are shown in Fig.8-10,

where ○ is defining position of perturbation variable and perturbation variables of ΔU, ΔV and ΔT_g are defined at the same position.

A typical triangular element e in Fig.8-10 is shown in Fig.11, where 4, 5 and 6 are middle points between sides. Perturbation variables represented as (33) are defined at node points and middle points between sides as shown in Fig.11. On the other hand, perturbation variables of ΔP and desired values represented as (34) are defined at node points.

$$\begin{aligned}
&\{\phi_{\Delta U}(t)\}^T = [\Delta U_1^e\ \Delta U_2^e\ \Delta U_3^e\ \Delta U_4^e\ \Delta U_5^e\ \Delta U_6^e]\\
&\{\phi_{\Delta V}(t)\}^T = [\Delta V_1^e\ \Delta V_2^e\ \Delta V_3^e\ \Delta V_4^e\ \Delta V_5^e\ \Delta V_6^e]\\
&\left\{\phi_{\Delta T_g}(t)\right\}^T = [\Delta T_{g1}^e\ \Delta T_{g2}^e\ \Delta T_{g3}^e\ \Delta T_{g4}^e\ \Delta T_{g5}^e\ \Delta T_{g6}^e]\\
&\{\phi_{\Delta T_s}(t)\}^T = [\Delta T_{s1}^e\ \Delta T_{s2}^e\ \Delta T_{s3}^e\ \Delta T_{s4}^e\ \Delta T_{s5}^e\ \Delta T_{s6}^e]
\end{aligned} \tag{33}$$

$$\begin{aligned}
&\{\phi_{\Delta P}(t)\}^T = [\Delta P_1^e\ \Delta P_2^e\ \Delta P_3^e]\\
&\{\phi_{U_r}\}^T = [U_{r1}^e\ U_{r2}^e\ U_{r3}^e]\\
&\{\phi_{V_r}\}^T = [V_{r1}^e\ V_{r2}^e\ V_{r3}^e]\\
&\left\{\phi_{T_{gr}}\right\}^T = [T_{gr1}^e\ T_{gr2}^e\ T_{gr3}^e]\\
&\{\phi_{T_{sr}}\}^T = [T_{sr1}^e\ T_{sr2}^e\ T_{sr3}^e]
\end{aligned} \tag{34}$$

The approximations of ΔU, ΔV, ΔT_g, ΔT_s, ΔP, U_r, V_r, T_{gr} and T_{sr} in element e are defined as

$$\begin{aligned}
&\Delta U^e = [\boldsymbol{M}]\{\phi_{\Delta U}(t)\}, \quad \Delta V^e = [\boldsymbol{M}]\{\phi_{\Delta V}(t)\}\\
&\Delta T_g^e = [\boldsymbol{M}]\left\{\phi_{\Delta T_g}(t)\right\}, \quad \Delta T_s^e = [\boldsymbol{M}]\{\phi_{\Delta T_s}(t)\}
\end{aligned} \tag{35}$$

$$\begin{aligned}
&\Delta P^e = [\boldsymbol{L}]\{\phi_{\Delta P}(t)\}\\
&U_r^e = [\boldsymbol{L}]\{\phi_{U_r}\}, \quad V_r^e = [\boldsymbol{L}]\{\phi_{V_r}\}\\
&T_{gr}^e = [\boldsymbol{L}]\left\{\phi_{T_{gr}}\right\}, \quad T_{sr}^e = [\boldsymbol{L}]\{\phi_{T_{sr}}\}
\end{aligned} \tag{36}$$

where $\boldsymbol{M}$ and $\boldsymbol{L}$ are

$$\begin{aligned}
[\boldsymbol{M}] = [&(2L_1-1)L_1\ (2L_2-1)L_2\ (2L_3-1)L_3\\
&4L_1L_2\quad 4L_2L_3\quad 4L_3L_1]
\end{aligned}$$

$$[\boldsymbol{L}] = [L_1\ L_2\ L_3]$$

$$L_1 = \frac{A_1}{\Delta^e}, \quad L_2 = \frac{A_2}{\Delta^e}, \quad L_3 = \frac{A_3}{\Delta^e}$$

$$\begin{aligned}
&A_1 = \frac{1}{2}\begin{vmatrix} 1 & x & y \\ 1 & x_2 & y_2 \\ 1 & x_3 & y_3 \end{vmatrix}, \quad A_2 = \frac{1}{2}\begin{vmatrix} 1 & x_1 & y_1 \\ 1 & x & y \\ 1 & x_3 & y_3 \end{vmatrix}\\
&A_3 = \frac{1}{2}\begin{vmatrix} 1 & x_1 & y_1 \\ 1 & x_2 & y_2 \\ 1 & x & y \end{vmatrix}, \quad \Delta^e = \frac{1}{2}\begin{vmatrix} 1 & x_1 & y_1 \\ 1 & x_2 & y_2 \\ 1 & x_3 & y_3 \end{vmatrix}
\end{aligned} \tag{37}$$

From (19)-(32), (35) and (36), the approximations are obtained by selecting a set of test functions $\boldsymbol{M}$ and $\boldsymbol{L}$ and by requiring that

$$\int\int_{\Delta^e} [\boldsymbol{L}]^T \left(\frac{\partial \Delta U^e}{\partial x} + \frac{\partial \Delta V^e}{\partial y}\right) dxdy = 0 \tag{38}$$

$$\begin{aligned}
\int\int_{\Delta^e} [\boldsymbol{M}]^T \Bigg(&\frac{\partial \Delta U^e}{\partial t} + \frac{\partial U_r^e}{\partial x}\Delta U^e + U_r^e\frac{\partial \Delta U^e}{\partial x}\\
&+\frac{\partial U_r^e}{\partial y}\Delta V^e + V_r^e\frac{\partial \Delta U^e}{\partial y} + \frac{\partial \Delta P^e}{\partial x}\\
&-\frac{1}{\mathrm{Re}}\left(\frac{\partial^2 \Delta U^e}{\partial x^2} + \frac{\partial^2 \Delta U^e}{\partial y^2}\right) + f_1\Delta U^e\\
&+f_2\frac{2U_r^{e2} + V_r^{e2}}{\sqrt{U_r^{e2} + V_r^{e2}}}\Delta U^e\\
&+f_2\frac{U_r^e V_r^e}{\sqrt{U_r^{e2} + V_r^{e2}}}\Delta V^e\Bigg) dxdy = 0
\end{aligned} \tag{39}$$

$$\begin{aligned}
\int\int_{\Delta^e} [\boldsymbol{M}]^T \Bigg(&\frac{\partial \Delta V^e}{\partial t} + \frac{\partial V_r^e}{\partial x}\Delta U^e + U_r^e\frac{\partial \Delta V^e}{\partial x}\\
&+\frac{\partial V_r^e}{\partial y}\Delta V^e + V_r^e\frac{\partial \Delta V^e}{\partial y} + \frac{\partial \Delta P^e}{\partial y}\\
&-\frac{1}{\mathrm{Re}}\left(\frac{\partial^2 \Delta V^e}{\partial x^2} + \frac{\partial^2 \Delta V^e}{\partial y^2}\right) + f_1\Delta V^e\\
&+f_2\frac{U_r^{e2} + 2V_r^{e2}}{\sqrt{U_r^{e2} + V_r^{e2}}}\Delta V^e\\
&+f_2\frac{U_r^e V_r^e}{\sqrt{U_r^{e2} + V_r^{e2}}}\Delta U^e\Bigg) dxdy = 0
\end{aligned} \tag{40}$$

$$\begin{aligned}
\int\int_{\Delta^e} [\boldsymbol{M}]^T \Bigg(&\frac{\partial \Delta T_g}{\partial t} + \frac{\partial T_g{}_r}{\partial x}\Delta U + U_r\frac{\partial \Delta T_g}{\partial x}\\
&+\frac{\partial T_g{}_r}{\partial y}\Delta V + V_r\frac{\partial \Delta T_g}{\partial y} - \frac{1}{\mathrm{RePr}}\left(\frac{\partial^2 \Delta T_g}{\partial x^2} + \frac{\partial^2 \Delta T_g}{\partial y^2}\right)\\
&+\alpha(\Delta T_g - \Delta T_s)\Bigg) dxdy = 0
\end{aligned} \tag{41}$$

$$\begin{aligned}
\int\int_{\Delta^e} [\boldsymbol{M}]^T \Bigg(&\frac{\partial \Delta T_s}{\partial t} - \beta\left(\frac{\partial^2 \Delta T_s}{\partial x^2} + \frac{\partial^2 \Delta T_s}{\partial y^2}\right)\\
&+\gamma(\Delta T_s - \Delta T_g) - \left.\frac{\partial f_3}{\partial U}\right|_{\substack{T_g=T_{gr}\\U=U_r\\V=V_r}}\Delta U - \left.\frac{\partial f_3}{\partial V}\right|_{\substack{T_g=T_{gr}\\U=U_r\\V=V_r}}\Delta V\\
&-\left.\frac{\partial f_3}{\partial T_g}\right|_{\substack{T_g=T_{gr}\\U=U_r\\V=V_r}}\Delta T_g\Bigg) dxdy = 0
\end{aligned} \tag{42}$$

where partial integral are used for (38), the seventh term of (39) and (40), the sixth term of (41) and the

second term of (42). The 4-6th terms of (42) are approximated by

$$\left.\frac{\partial f_3}{\partial U}\right|_{\substack{T_g=T_{gr}\\U=U_r\\V=V_r}} = [\boldsymbol{L}]\times \left[\begin{array}{ccc} \left.\frac{\partial f_3}{\partial U}\right|_{\substack{T_g=T_{gr1}^e\\U=U_{r1}^e\\V=V_{r1}^e}} & \left.\frac{\partial f_3}{\partial U}\right|_{\substack{T_g=T_{gr2}^e\\U=U_{r2}^e\\V=V_{r2}^e}} & \left.\frac{\partial f_3}{\partial U}\right|_{\substack{T_g=T_{gr3}^e\\U=U_{r3}^e\\V=V_{r3}^e}} \end{array}\right]^T$$

$$\left.\frac{\partial f_3}{\partial V}\right|_{\substack{T_g=T_{gr}\\U=U_r\\V=V_r}} = [\boldsymbol{L}]\times \left[\begin{array}{ccc} \left.\frac{\partial f_3}{\partial V}\right|_{\substack{T_g=T_{gr1}^e\\U=U_{r1}^e\\V=V_{r1}^e}} & \left.\frac{\partial f_3}{\partial V}\right|_{\substack{T_g=T_{gr2}^e\\U=U_{r2}^e\\V=V_{r2}^e}} & \left.\frac{\partial f_3}{\partial V}\right|_{\substack{T_g=T_{gr3}^e\\U=U_{r3}^e\\V=V_{r3}^e}} \end{array}\right]^T$$

$$\left.\frac{\partial f_3}{\partial T_g}\right|_{\substack{T_g=T_{gr}\\U=U_r\\V=V_r}} = [\boldsymbol{L}]\times \left[\begin{array}{ccc} \left.\frac{\partial f_3}{\partial T_g}\right|_{\substack{T_g=T_{gr1}^e\\U=U_{r1}^e\\V=V_{r1}^e}} & \left.\frac{\partial f_3}{\partial T_g}\right|_{\substack{T_g=T_{gr2}^e\\U=U_{r2}^e\\V=V_{r2}^e}} & \left.\frac{\partial f_3}{\partial T_g}\right|_{\substack{T_g=T_{gr3}^e\\U=U_{r3}^e\\V=V_{r3}^e}} \end{array}\right]^T \quad (43)$$

From (38)-(43), consider all triangular elements in Fig.8-10 and boundary conditions, that is

$$\begin{aligned}
&\Delta U_i = 0 \ (i: \text{number at wall})\\
&\Delta V_i = 0 \ (i: \text{number at wall})\\
&\Delta P_i = 0 \ (i = 2)\\
&\Delta U_{26} = \Delta U_{\text{in}1}, \quad \Delta U_{30} = \Delta U_{\text{in}2},\\
&\Delta V_{32} = \Delta V_{\text{in}1}, \quad \Delta V_{34} = \Delta V_{\text{in}2}\\
&\Delta T_{g\ 26} = 0, \quad \Delta T_{g\ 30} = 0,\\
&\Delta T_{g\ 32} = 0, \quad \Delta T_{g\ 34} = 0
\end{aligned} \quad (44)$$

and suppose that state vector $\boldsymbol{x}$: (99×1) and control vector $\boldsymbol{u}$: (4×1) are

$$\begin{aligned}
&\boldsymbol{x} = [\boldsymbol{x_1}\ \boldsymbol{x_2}]^T \ (99\times 1)\\
&\boldsymbol{x_1} = [\boldsymbol{x_{11}}\ \boldsymbol{x_{21}}\ \boldsymbol{x_{31}}\ \boldsymbol{x_{41}}] \ (88\times 1)\\
&\boldsymbol{x_2} = [\Delta P_1\ \Delta P_3\ \cdots\ \Delta P_{12}] \ (11\times 1)\\
&\boldsymbol{x_{11}} = [\Delta T_{g1}\ \cdots\ \Delta T_{g25}\ \Delta T_{g27}\ \Delta T_{g28}\\
&\qquad \Delta T_{g29}\ \Delta T_{g31}\ \Delta T_{g33}\ \Delta T_{g35}] \ (31\times 1)\\
&\boldsymbol{x_{21}} = [\Delta T_{s1}\ \cdots\ \Delta T_{s25}] \ (25\times 1)\\
&\boldsymbol{x_{31}} = [\Delta U_3\ \Delta U_7\ \Delta U_8\ \Delta U_9\ \cdots\\
&\qquad \Delta U_{27}\ \Delta U_{28}\ \Delta U_{29}] \ (16\times 1)\\
&\boldsymbol{x_{41}} = [\Delta V_3\ \Delta V_7\ \Delta V_8\ \Delta V_9\ \cdots\\
&\qquad \Delta V_{27}\ \Delta V_{28}\ \Delta V_{29}] \ (16\times 1)\\
&\boldsymbol{u} = [\Delta U_{\text{in}1}\ \ \Delta U_{\text{in}2}\ \ \Delta V_{\text{in}1}\ \ \Delta V_{\text{in}2}]^T, \ (4\times 1)
\end{aligned} \quad (45)$$

we get

$$\begin{aligned}
&\boldsymbol{E}\dot{\boldsymbol{x}} = \boldsymbol{A}\boldsymbol{x} + \boldsymbol{B}\boldsymbol{u} \ : \ \boldsymbol{E}(99\times 99),\ \boldsymbol{A}(99\times 99),\ \boldsymbol{B}(99\times 8)\\
&\boldsymbol{x} = \left[\begin{array}{c} \boldsymbol{x_1}\\ \boldsymbol{x_2}\end{array}\right], \quad \boldsymbol{E} = \left[\begin{array}{cc} \boldsymbol{E_{11}} & \boldsymbol{0}\\ \boldsymbol{0} & \boldsymbol{0}\end{array}\right]\\
&\boldsymbol{A} = \left[\begin{array}{cc} \boldsymbol{A_{11}} & \boldsymbol{A_{12}}\\ \boldsymbol{A_{21}} & \boldsymbol{A_{22}}\end{array}\right], \quad \boldsymbol{B} = \left[\begin{array}{c} \boldsymbol{B_1}\\ \boldsymbol{B_2}\end{array}\right]
\end{aligned} \quad (46)$$

where $\boldsymbol{A_{22}} = \boldsymbol{0}$. Since $\boldsymbol{E}$ isn't nonsingular matrix, (46) isn't called state equation used widely in control design. Equation (46) is called descriptor system[14]. Descriptor system is constructed because there aren't temporal differentiation of ΔP in (19)-(21).

If descriptor system of (46) is impulse controllable and finite dynamics stabilizable, it is possible to design control system[14]. But, equation (46) isn't impulse controllable. So, in the following subsection, we will transform descriptor system of (46) into state equation by using generalized inverse matrix[15] so that control system can be designed.

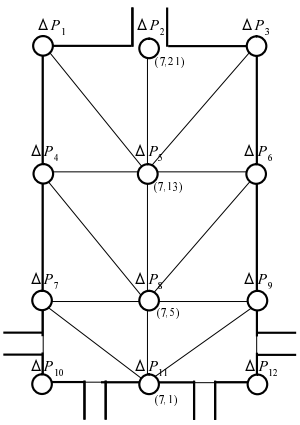

Fig. 8: Perturbation variables of ΔP

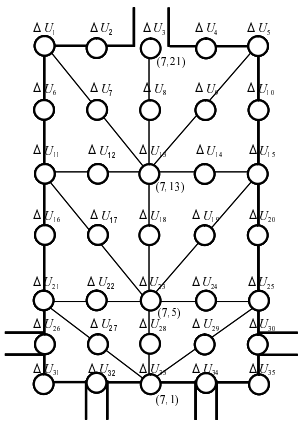

Fig. 9: Perturbation variables of ΔU

3.3 Application of Generalized Inverse Matrix to Descriptor System[15]

From (46), we get

$$\boldsymbol{A_{22}}\boldsymbol{x_2} = -\boldsymbol{A_{21}}\boldsymbol{x_1} - \boldsymbol{B_2}\boldsymbol{u} \quad (47)$$

Since $\boldsymbol{A_{22}} = \boldsymbol{0}$, generalized inverse matrix $\boldsymbol{A_{22}}^\sharp$ of $\boldsymbol{A_{22}}$ is $\boldsymbol{0}$. So, from (46) and (47) we have that

$$\boldsymbol{x_2} = \boldsymbol{A_{22}}^\sharp(-\boldsymbol{A_{21}}\boldsymbol{x_1} - \boldsymbol{B_2}\boldsymbol{u}) = \boldsymbol{0} \quad (48)$$

and inserting into (46), we get the state equation

$$\dot{\boldsymbol{x_1}} = \boldsymbol{E_{11}}^{-1}\boldsymbol{A_{11}}\boldsymbol{x_1} + \boldsymbol{E_{11}}^{-1}\boldsymbol{B_1}\boldsymbol{u} \quad (49)$$

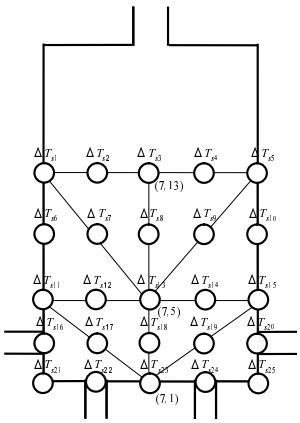

Fig. 10: Perturbation variables of ΔT_s

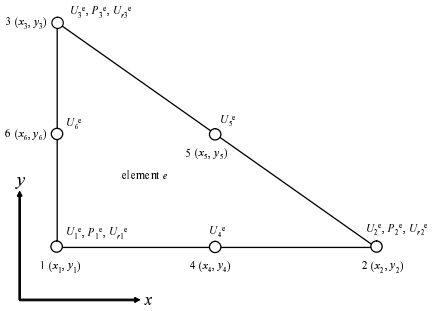

Fig. 11: A typical triangular element

and suppose that $\boldsymbol{E_{11}}^{-1}\boldsymbol{A_{11}}$ is $\boldsymbol{A}$ and $\boldsymbol{E_{11}}^{-1}\boldsymbol{B_1}$ is $\boldsymbol{B}$ and consider instrument placement shown in Fig.3, we get the state space model

$$
\begin{aligned}
&\dot{\boldsymbol{x}} = \boldsymbol{A}\boldsymbol{x} + \boldsymbol{B}\boldsymbol{u} \ : \ \boldsymbol{A}(88\times 88),\ \boldsymbol{B}(88\times 8)\\
&\boldsymbol{y} = \boldsymbol{C}\boldsymbol{x} \ : \ \boldsymbol{C}(13\times 88)\\
&\boldsymbol{x} = \boldsymbol{x_1}^T \ (13\times 1)\\
&\boldsymbol{u} = [\Delta U_{\rm in1} \ \ \Delta U_{\rm in2} \ \ \Delta V_{\rm in1} \ \ \Delta V_{\rm in2}]^T \ (4\times 1)\\
&\boldsymbol{y} = [\Delta T_{s1} \ \cdots \ \Delta T_{s6} \ \Delta T_{s10} \ \Delta T_{s11}\\
&\qquad \Delta T_{s15} \ \Delta T_{s21} \ \Delta T_{s25} \ \Delta U_3 \ \Delta V_3]^T \ (13\times 1)
\end{aligned}
\tag{50}
$$

Since (50) is stabilizable and detectable[9], linear control theory becomes available.

4 CONTROL SYSTEM OF REACTOR FURNACE

LQG control[10] is adopted in order to dealt with problem description in next section. The detailed explanation of LQG control is given in appendix B.

LQG control system of reactor furnace model is shown in Fig.12. LQG control system is constructed by (50), where $\boldsymbol{K}$ is optimal regulator gain, $\boldsymbol{L}$ is kalman filter gain, $\hat{\boldsymbol{x}}$ is estimated internal state value of reactor furnace model. In the following, flow of control is shown.

Step1 Inner state variables of reactor furnace model are estimated by kalman filter and the measured data of instrumentations shown in Fig.3.

Step2 Based on optimal regulator and inner state variables estimated in Step1, velocity of blowing gases from tuyeres is modified in order to match initial distribution of reactor furnace model to desired one.

where velocity of blowing gases from tuyeres is ($U_{\rm in1}$, $U_{\rm in2}$, $V_{\rm in1}$, $V_{\rm in2}$), initial distribution is ($P(x,y,0)$, $\boldsymbol{V}(x,y,0)$, $T_g(x,y,0)$, $T_s(x,y,0)$), desired distribution is ($P_r(x,y)$, $\boldsymbol{V}_r(x,y)$, $T_{g\,r}(x,y)$, $T_{s\,r}(x,y)$) and (P_r, $\boldsymbol{V}_r$, $T_{g\,r}$, $T_{s\,r}$) is a steady state solution of (2)-(16).

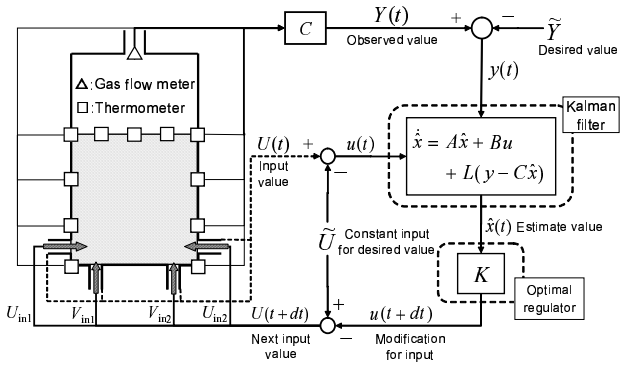

Fig. 12: LQG optimal control system

5 NUMERICAL EXPERIMENT

In this research, temperature distribution control of reactor furnace model is aimed by using reactor furnace model constructed in section 2. In this section, numerical results of LQG control are shown. Problem description is shown in the following.

- Velocity ($U_{\rm in1}$, $U_{\rm in2}$, $V_{\rm in1}$, $V_{\rm in2}$) of blowing gases from tuyeres is decided so that initial distribution ($P(x,y,0)$, $\boldsymbol{V}(x,y,0)$, $T_g(x,y,0)$, $T_s(x,y,0)$) in Fig.13-16 can be controlled to desired distribution (P_r, $\boldsymbol{V}_r$, $T_{g\,r}$, $T_{s\,r}$) in Fig.4-7.

Initial temperature distribution in Fig.15 and 16 is higher than desired one in Fig.6 and 7 totally.

Suppose that $\boldsymbol{Q}$, $\boldsymbol{W}$, $\boldsymbol{R}$ and $\boldsymbol{V}$ of appendix B are

$$\boldsymbol{Q} = \boldsymbol{W} = \mathrm{diag}(\overbrace{10,\ \cdots,\ 10}^{56\ \text{elements}}\ \overbrace{0.1,\ \cdots,\ 0.1}^{32\ \text{elements}}) \ :\ (88\times 88)$$

$$\boldsymbol{R} = \boldsymbol{V} = 7.0\times 10^6 \times \mathrm{diag}(1,\ 1,\ 1,\ 1) \ :\ (4\times 4)$$

Since the purposes of this research is to estimate inner temperature values of reactor furnace model and to match temperature distribution of reactor furnace model to desired one, two objective functions are defined as

$$\hat{f}(t) = \sum_{\substack{i=1\\ i\neq 26,30,32,34}}^{35} |T_{gi}(t) - \hat{T}_{gi}(t)| + \sum_{i=1}^{25} |T_{si}(t) - \hat{T}_{si}(t)| \qquad (51)$$

where $T_{gi}(t)$ and $T_{si}(t)$ are temperature values of reactor furnace model at node points of Fig.9 and 10, $\hat{T}_{gi}(t)$ and $\hat{T}_{si}(t)$ are estimated temperature values by LQG control at above points. Equation (51) represents error estimator of temperature values at above points.

$$f(t) = \sum_{i=1}^{13}\sum_{j=1}^{21} |T_{g\ i,j}^{\ n} - T_{g\ i,j}^{r}| + \sum_{i=1}^{13}\sum_{j=1}^{13} |T_{s\ i,j}^{\ n} - T_{s\ i,j}^{r}| \qquad (52)$$

where $T_{g\ i,j}^{r}$ and $T_{s\ i,j}^{r}$ are desired temperature values at (i,j). Equation (52) represents error of temperature values at all node points.

The velocity changes of blowing gases from tuyeres are shown in Fig.17 and 18. The changes of the two objective functions are shown in Fig.19. From Fig.17 and 18, the velocity of blowing gases from tuyeres is operated in about 15[-]. When gases blow from tuyeres as shown in Fig.17 and 18, the two objective functions decrease with time. The optimized temperature distribution is shown in Fig.20 and 21. So, inner temperature values of reactor furnace model are estimated and temperature distribution approaches the desired one by using LQG control system.

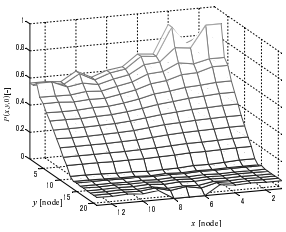

Fig. 13: Initial distribution of pressure

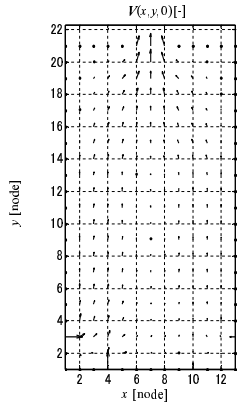

Fig. 14: Initial distribution of gas flow

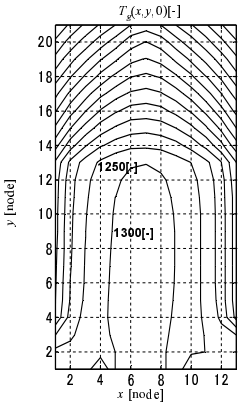

Fig. 15: Initial distribution of gas temperature

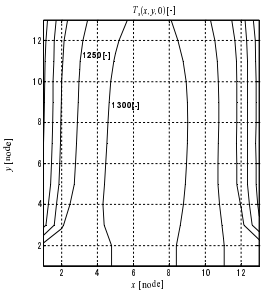

Fig. 16: Initial distribution of material temperature

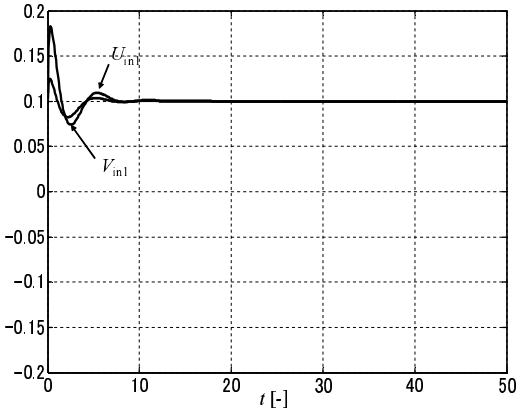

Fig. 17: $U_{\mathrm{in}1}$ and $V_{\mathrm{in}1}$

6 CONCLUSION

In this paper, the reactor furnace simulator was constructed, which could calculate gas temperature, solid temperature, gas flow and pressure distribution in the furnace. The simulator had instrumentations only near the furnace wall and control inputs at only bound-

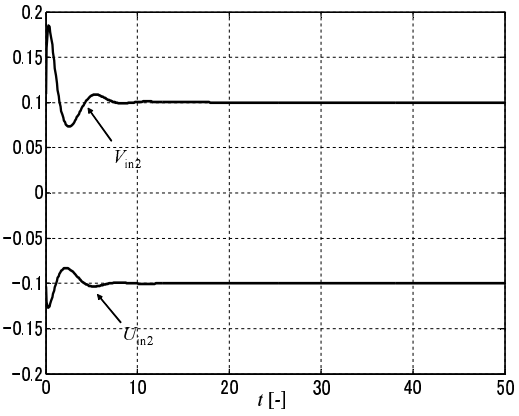

Fig. 18: $U_{\mathrm{in}2}$ and $V_{\mathrm{in}2}$

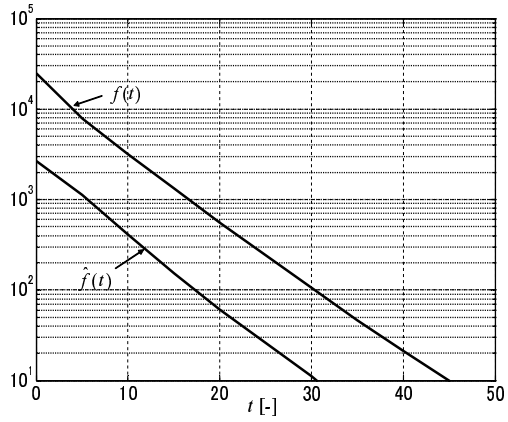

Fig. 19: Changes of $\hat{f}(t)$ and $f(t)$

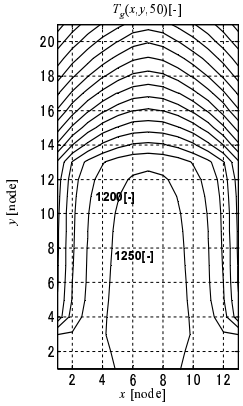

Fig. 20: The optimized distribution of gas temperature($t = 50[-]$)

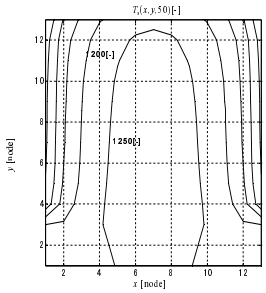

Fig. 21: The optimized distribution of material temperature($t = 50[-]$)

aries. To make the control system design, state space model was derived by applying FEM to the simulator. Through this procedure, linear control theory could be applied for design of control system. Further, LQG control was adopted in order to deal with the problem description. We confirmed that temperature distribution of the simulator was estimated and controlled by LQG control system.

In the future, it will be necessary to improve estimated inner temperature values and regulate temperature distribution to the desired one in a short time. For the purpose, we will adopt other linear control theories such as H^2 control and H^∞ control.

REFERENCES

[1] T. Kawamura: Fluid analysis I, Asakura shoten (1996), 1-83.

[2] T. Shibuta: Master Thesis. Okayama Univ., (2003)

[3] K. Ishimaru: Master Thesis. Okayama Univ., (2005)

[4] T. Takeda: Graduation Thesis. Okayama Univ., (2006)

[5] K. Takatani, T. Inada and K. Takata: ISIJ International, **41**-10 (2001), 1139-1145.

[6] I. Imai: Fluid Dynamics, Shokabo (1973), 259-284.

[7] S. Ergun: Chemical Engineering Progress, **48**-2 (1952), 89-94.

[8] M. Iri and Y. Iri: Partial Differential Equation, Asakura shoten (1983), 13-35.

[9] K. Z. Liu: Linear Robust Control, Coronasha (2002), 78-179.

[10] S. Hosoe: System and Control, Ohmsha (1997), 97-110

[11] A. Fujimori: Robust Control, Coronasha (2001), 42-139.

[12] O. M. Aamo and M. Krstic: Flow Control by Feedback, Springer (2003), 14-17.

[13] G. Yagawa: Beginning FEM of Flow and Heat Transfer, Baifukan (1983), 86-170.

[14] T. Katayama: Optimal Control of Linear System, Kindai Kagaku sha (1999), 125-180.

[15] H. Kimura: Linear Algebra, University of Tokyo Press (2003), 112-114.

Appendix A

In this research, finite-difference method is used to calculate gas flow and temperature distribution of reactor furnace model. Flow chart of the calculation is shown in Fig.22. The gas flow is calculated by MAC method. These calculations are continued until the convergence conditions are fulfilled. The convergence conditions are defined as

$$
\begin{aligned}
f_P &= \max|P(x,y,n_P) - P(x,y,n_P-1)| < 0.0001 \\
&\qquad (n_P = 1,2\cdots) \\
f_U &= \max|U(x,y,n_V) - U(x,y,n_V-1)| < 0.0001 \\
&\qquad (n_V = 1,2\cdots) \\
f_V &= \max|V(x,y,n_V) - V(x,y,n_V-1)| < 0.0001 \\
&\qquad (n_V = 1,2\cdots) \\
f_{T_g} &= \max|T_g(x,y,10n_{T_g}) - T_g(x,y,10(n_{T_g}-1))| < 0.1 \\
&\qquad (n_{T_g} = 1,2\cdots) \\
f_{T_s} &= \max|T_s(x,y,10n_{T_s}) - T_s(x,y,10(n_{T_s}-1))| < 0.1 \\
&\qquad (n_{T_s} = 1,2\cdots) \qquad (53)
\end{aligned}
$$

The conditions are shown in Fig.23-25, Table.3 and 4 in order to get a steady state solution of Fig.4-7 in subsection 3.1. Reactor furnace model calculates the discrete values in Table.2 at $dt(=0.01)$ intervals under the conditions of Table.3.

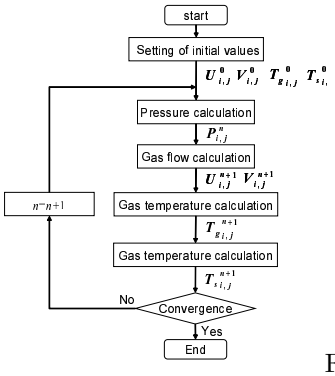

Fig. 22: Flow chart to calculate mathematical model

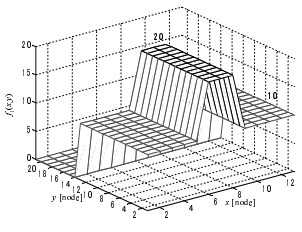

Fig. 23: Condition of f_1 for desired distribution

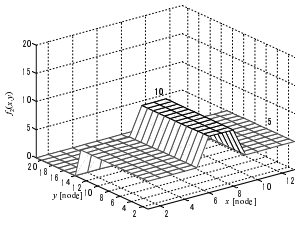

Fig. 24: Condition of f_2 for desired distribution

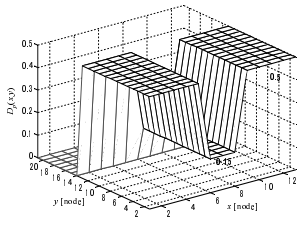

Fig. 25: Condition of D_p for desired distribution

Table. 3: Condition 1 of desired distribution

dt	0.01	b_{up}	1
$dx,\ dy$	0.1	T_{out}	20
Re	100	Q_1	10000
Pr	0.5	Q_2	1000
$\alpha,\ \gamma$	10	K_1	50
β	0.01	E	50000
$a,\ b$	1	R	8.31

Table. 4: Condition 2 of desired distribution

U_{in1}, V_{in1}, V_{in2}	0.1
U_{in2}	-0.1
$T_{g\ \mathrm{in1}}$, $T_{g\ \mathrm{in2}}$, $T_{g\ \mathrm{in3}}$, $T_{g\ \mathrm{in4}}$	1200
$U^0_{i,j}$, $V^0_{i,j}$ (except inlet)	0
$T_{g\ i,j}^{\ 0}$ (except inlet)	20
$T_{s\ i,j}^{\ 0}$	20

Appendix B

In LQG control, state space model is assumed to be subjected to disturbances entering additively in equation. Thus, we have

$$
\begin{aligned}
&\dot{\boldsymbol{x}} = \boldsymbol{A}\boldsymbol{x} + \boldsymbol{B}\boldsymbol{u} + \boldsymbol{w} \ :\ \boldsymbol{A}(n\times n),\ \boldsymbol{B}(m\times n) \\
&\boldsymbol{y} = \boldsymbol{C}\boldsymbol{x} + \boldsymbol{v} \ :\ \boldsymbol{C}(l\times n) \qquad (54)
\end{aligned}
$$

where $\boldsymbol{w}$ is a disturbance and $\boldsymbol{v}$ is measurement noise. $\boldsymbol{w}$ and $\boldsymbol{v}$ are assumed to be uncorrelated Gaussian

stochastic processes with zero means and covariance

$$E\{\boldsymbol{w}(t)\} = \boldsymbol{0}, \quad E\{\boldsymbol{v}(t)\} = \boldsymbol{0}$$
$$E\left\{ \begin{bmatrix} \boldsymbol{w}(t) \\ \boldsymbol{v}(t) \end{bmatrix} \begin{bmatrix} \boldsymbol{w}(\tau)^T & \boldsymbol{v}(\tau)^T \end{bmatrix} \right\} = \begin{bmatrix} \boldsymbol{W} & \boldsymbol{0} \\ \boldsymbol{0} & \boldsymbol{V} \end{bmatrix} \delta(t-\tau) \tag{55}$$

respectively, where $\boldsymbol{W}$ and $\boldsymbol{V}$ are constant matrices. $E\{\cdot\}$ denotes the expectation operator and δ denotes the delta function. The LQG control problem is to find the feedback $\boldsymbol{u}$ that minimizes the cost functional

$$J = E\left\{ \lim_{T\to\infty} \frac{1}{T} \int_{t_0}^{T} \left(\boldsymbol{x}^T \boldsymbol{Q} \boldsymbol{x} + \boldsymbol{u}^T \boldsymbol{R} \boldsymbol{u} \right) dt \right\} \tag{56}$$

where $\boldsymbol{Q}$ and $\boldsymbol{R}$ are constant weighting matrices satisfying $\boldsymbol{Q} = \boldsymbol{Q}^T \geq 0$ and $\boldsymbol{R} = \boldsymbol{R}^T > 0$. The problem has a unique solution given by

$$\begin{aligned} &\boldsymbol{u} = -\boldsymbol{K}\hat{\boldsymbol{x}}, \quad \boldsymbol{K} = \boldsymbol{R^{-1}B^T P} \\ &\dot{\hat{\boldsymbol{x}}} = \boldsymbol{A}\hat{\boldsymbol{x}} + \boldsymbol{B}\boldsymbol{u} + \boldsymbol{L}(\boldsymbol{y} - \boldsymbol{C}\hat{\boldsymbol{x}}), \\ &\boldsymbol{L} = \boldsymbol{SC^T V^{-1}}, \quad \hat{\boldsymbol{x}}(t_0) = \boldsymbol{0} \end{aligned} \tag{57}$$

where $\boldsymbol{P}$ and $\boldsymbol{S}$ uniquely solve the algebraic Riccati equations

$$\begin{aligned} &\boldsymbol{A}^T\boldsymbol{P} + \boldsymbol{P}\boldsymbol{A} + \boldsymbol{Q} - \boldsymbol{P}\boldsymbol{B}\boldsymbol{R}^{-1}\boldsymbol{B}^T\boldsymbol{P} = \boldsymbol{0}, \\ &\boldsymbol{A}\boldsymbol{S} + \boldsymbol{S}\boldsymbol{A}^T + \boldsymbol{W} - \boldsymbol{S}\boldsymbol{C}^T\boldsymbol{V}^{-1}\boldsymbol{C}\boldsymbol{S} = \boldsymbol{0}. \end{aligned} \tag{58}$$

We show that there exists an admissible LQG control system, if the following two conditions hold

(A.1) $(\boldsymbol{A},\boldsymbol{B})$ and $(\boldsymbol{A}^T,\boldsymbol{C}^T)$ are stabilizable, that is

$$\begin{aligned} &\mathrm{rank}[s\boldsymbol{I} - \boldsymbol{A} \quad \boldsymbol{B}] = n, \quad \mathrm{rank}[s\boldsymbol{I} - \boldsymbol{A}^T \quad \boldsymbol{C}^T] = n, \\ &\mathrm{Re}[s] \geq 0, \quad s \in \mathbb{C} \end{aligned} \tag{59}$$

(A.2) $(\sqrt{\boldsymbol{Q}},\boldsymbol{A})$ and $(\sqrt{\boldsymbol{W}},\boldsymbol{A}^T)$ are detectable, that is

$$\begin{aligned} &\mathrm{rank}\begin{bmatrix} s\boldsymbol{I} - \boldsymbol{A} \\ \sqrt{\boldsymbol{Q}} \end{bmatrix} = n, \quad \mathrm{rank}\begin{bmatrix} s\boldsymbol{I} - \boldsymbol{A}^T \\ \sqrt{\boldsymbol{W}} \end{bmatrix} = n, \\ &\mathrm{Re}[s] \geq 0, \quad s \in \mathbb{C} \end{aligned} \tag{60}$$